Research Article | Vol. 9, No. 7 | 1 Jul 2018 | BIOMEDICAL OPTICS EXPRESS 3373
Biomedical Optics EXPRESS

New fluorescent compounds produced by femtosecond laser surgery in biological tissues: the mechanisms

ZHONGYA QIN,[1,4] QIQI SUN,[1,4] YUE LIN,[2] SICONG HE,[1] XUESONG LI,[1] CONGPING CHEN,[1] WANJIE WU,[1] YI LUO,[2] AND JIANAN Y. QU[1,3,*]

[1]*Department of Electronic and Computer Engineering, Hong Kong University of Science and Technology, Clear Water Bay, Kowloon, Hong Kong SAR, China*
[2]*Bio-X Division, Hefei National Laboratory for Physical Science at the Microscale, University of Science and Technology of China, Hefei, Anhui, China*
[3]*Center of Systems Biology and Human Health, School of Science and Institute for Advanced Study, Hong Kong University of Science and Technology, Clear Water Bay, Kowloon, Hong Kong SAR, China*
[4]*These authors contributed equally to this work*
**eequ@ust.hk*

Abstract: The femtosecond laser ablation in biological tissue produces highly fluorescent compounds that are of great significance for intrinsically labelling ablated tissue *in vivo* and achieving imaging-guided laser microsurgery. In this study, we analyzed the molecular structures of femtosecond laser-ablated tissues using Raman spectroscopy and transmission electron microscopy. The results showed that though laser ablation caused carbonization, no highly fluorescent nanostructures were found in the ablated tissues. Further, we found that the fluorescence properties of the newly formed compounds were spatially heterogeneous across the ablation site and the dominant fluorescent signals exhibited close similarity to the tissue directly heated at a temperature of 200 °C. The findings of our study indicated that the new fluorescent compounds were produced via the laser heating effect and their formation mechanism likely originated from the Maillard reaction, a chemical reaction between amino acids and reducing sugars in tissue.

OCIS codes: (170.1020) Ablation of tissue; (140.7090) Ultrafast lasers; (180.4315) Nonlinear microscopy; (300.6500) Spectroscopy, time-resolved; (170.5660) Raman spectroscopy.

References and links

1. B.-G. Wang, I. Riemann, H. Schubert, K.-J. Halbhuber, and K. Koenig, "In-vivo intratissue ablation by nanojoule near-infrared femtosecond laser pulses," Cell Tissue Res. **328**(3), 515–520 (2007).
2. A. Vogel, J. Noack, G. Hüttman, and G. Paltauf, "Mechanisms of femtosecond laser nanosurgery of cells and tissues," Appl. Phys. B **81**(8), 1015–1047 (2005).
3. P. S. Tsai and D. Kleinfeld, "In vivo two-photon laser scanning microscopy with concurrent plasma-mediated ablation principles and hardware realization," in *In Vivo Optical Imaging of Brain Function* (CRC Press, 2009).
4. K. Koenig, O. Krauss, and I. Riemann, "Intratissue surgery with 80 MHz nanojoule femtosecond laser pulses in the near infrared," Opt. Express **10**(3), 171–176 (2002).
5. A. K. N. Thayil, A. Pereira, M. Mathew, D. Artigas, E. M. Blanco, and P. Loza-Alvarez, "Decrease in laser ablation threshold for epithelial tissue microsurgery in a living Drosophila embryo during dorsal closure," J. Microsc. **232**(2), 362–368 (2008).
6. V. Hovhannisyan, W. Lo, C. Hu, S.-J. Chen, and C. Y. Dong, "Dynamics of femtosecond laser photo-modification of collagen fibers," Opt. Express **16**(11), 7958–7968 (2008).
7. Q. Sun, Z. Qin, W. Wu, Y. Lin, C. Chen, S. He, X. Li, Z. Wu, Y. Luo, and J. Y. Qu, "In vivo imaging-guided microsurgery based on femtosecond laser produced new fluorescent compounds in biological tissues," Biomed. Opt. Express **9**(2), 581–590 (2018).
8. Q. Yang, L. Wei, X. Zheng, and L. Xiao, "Single particle dynamic imaging and Fe^{3+} sensing with bright carbon dots derived from bovine serum albumin proteins," Sci. Rep. **5**(1), 17727 (2016).
9. K. R. Millington, H. Ishii, and G. Maurdev, "Chemiluminescence from thermal oxidation of amino acids and proteins," Amino Acids **38**(5), 1395–1405 (2010).
10. S. Zhu, J. Zhang, L. Wang, Y. Song, G. Zhang, H. Wang, and B. Yang, "A general route to make non-conjugated linear polymers luminescent," Chem. Commun. (Camb.) **48**(88), 10889–10891 (2012).

#328072 https://doi.org/10.1364/BOE.9.003373
Journal © 2018 Received 16 Apr 2018; revised 14 Jun 2018; accepted 19 Jun 2018; published 26 Jun 2018

Biomedical Optics EXPRESS

11. I. Maxwell, "Application of femtosecond lasers for subcellular nanosurgery," PhD Thesis (2006).
12. C. B. Schaffer, J. F. García, and E. Mazur, "Bulk heating of transparent materials using a high-repetition-rate femtosecond laser," Appl. Phys., A Mater. Sci. Process. **76**(3), 351–354 (2003).
13. A. Cao, A. K. Pandya, G. K. Serhatkulu, R. E. Weber, H. Dai, J. S. Thakur, V. M. Naik, R. Naik, G. W. Auner, R. Rabah, and D. C. Freeman, "A robust method for automated background subtraction of tissue fluorescence," J. Raman Spectrosc. **38**(9), 1199–1205 (2007).
14. M. Nakamizo, R. Kammereck, and P. L. Walker, Jr., "Laser Raman studies on carbons," Carbon **12**(3), 259–267 (1974).
15. R. Galli, O. Uckermann, E. F. Andresen, K. D. Geiger, E. Koch, G. Schackert, G. Steiner, and M. Kirsch, "Intrinsic indicator of photodamage during label-free multiphoton microscopy of cells and tissues," PLoS One **9**(10), e110295 (2014).
16. N. Morita, Y. Shimotsuma, M. Nishi, M. Sakakura, K. Miura, and K. Hirao, "Direct micro-carbonization inside polymer using focused femtosecond laser pulses," Appl. Phys. Lett. **105**(20), 201104 (2014).
17. R. Rahimi, M. Ochoa, W. Yu, and B. Ziaie, "Highly stretchable and sensitive unidirectional strain sensor via laser carbonization," ACS Appl. Mater. Interfaces **7**(8), 4463–4470 (2015).
18. S. Y. Cho, Y. S. Yun, S. Lee, D. Jang, K.-Y. Park, J. K. Kim, B. H. Kim, K. Kang, D. L. Kaplan, and H.-J. Jin, "Carbonization of a stable β-sheet-rich silk protein into a pseudographitic pyroprotein," Nat. Commun. **6**(1), 7145 (2015).
19. S. N. Baker and G. A. Baker, "Luminescent carbon nanodots: emergent nanolights," Angew. Chem. Int. Ed. Engl. **49**(38), 6726–6744 (2010).
20. X. T. Zheng, A. Ananthanarayanan, K. Q. Luo, and P. Chen, "Glowing graphene quantum dots and carbon dots: properties, syntheses, and biological applications," Small **11**(14), 1620–1636 (2015).
21. S. Zhu, Y. Song, X. Zhao, J. Shao, J. Zhang, and B. Yang, "The photoluminescence mechanism in carbon dots (graphene quantum dots, carbon nanodots, and polymer dots): current state and future perspective," Nano Res. **8**(2), 355–381 (2015).
22. X. Wang, K. Qu, B. Xu, J. Ren, and X. Qu, "Microwave assisted one-step green synthesis of cell-permeable multicolor photoluminescent carbon dots without surface passivation reagents," J. Mater. Chem. **21**(8), 2445 (2011).
23. C. G. A. Davies and T. P. Labuza, "The Maillard reaction: application to confectionery products," in *Confectionary Science, International Symposium on,* (1997), pp. 35–66.
24. H.-Y. Wang, H. Qian, and W.-R. Yao, "Melanoidins produced by the Maillard reaction: Structure and biological activity," Food Chem. **128**(3), 573–584 (2011).
25. H. E. Nursten, *The Maillard Reaction: Chemistry, Biochemistry and Implications* (Royal Society of Chemistry, 2007).
26. P. Naik, *Biochemistry* (Jaypee Brothers,Medical Publishers Pvt. Limited, 2015).
27. S. Zhu, Y. Song, J. Shao, X. Zhao, and B. Yang, "Non-conjugated polymer dots with crosslink-enhanced emission in the absence of fluorophore units," Angew. Chem. Int. Ed. Engl. **54**(49), 14626–14637 (2015).
28. W. Li, Z. Zhang, B. Kong, S. Feng, J. Wang, L. Wang, J. Yang, F. Zhang, P. Wu, and D. Zhao, "Simple and green synthesis of nitrogen-doped photoluminescent carbonaceous nanospheres for bioimaging," Angew. Chem. Int. Ed. Engl. **52**(31), 8151–8155 (2013).
29. T. Lai, E. Zheng, L. Chen, X. Wang, L. Kong, C. You, Y. Ruan, and X. Weng, "Hybrid carbon source for producing nitrogen-doped polymer nanodots: one-pot hydrothermal synthesis, fluorescence enhancement and highly selective detection of Fe(III)," Nanoscale **5**(17), 8015–8021 (2013).
30. Y. Yang, J. Cui, M. Zheng, C. Hu, S. Tan, Y. Xiao, Q. Yang, and Y. Liu, "One-step synthesis of amino-functionalized fluorescent carbon nanoparticles by hydrothermal carbonization of chitosan," Chem. Commun. (Camb.) **48**(3), 380–382 (2012).

1. Introduction

Laser surgery has been widely used for precise ablation of targeted biological tissues [1]. Due to the highly localized nonlinear photo-ionization process, femtosecond laser surgery provides a considerably better spatial precision in tissue ablation than that of continuous-wave or long-pulsed irradiation [2]. Interestingly, it has been reported that the biological tissues such as brain tissue of rats [3], porcine cornea [4], epithelial tissue of *Drosophila* embryos [5] and bovine tendon collagen [6] became highly fluorescent after ablation using a femtosecond laser of high repetition rate. Therefore, sharing the same femtosecond laser source, it is desirable to combine the laser ablation with a multiphoton fluorescence microscopy and to achieve imaging-guided laser microsurgery [3]. Recently, we have demonstrated laser microsurgery guided by the two-photon fluorescence microscopy in a variety of tissues *in vivo* [7]. The results showed that the fluorescent compounds produced by the femtosecond laser are of great significance for intrinsically labelling ablated tissue *in vivo*. Furthermore, we characterized the fluorescence properties of the femtosecond laser ablated biological

Biomedical Optics EXPRESS

samples and found that the fluorescent compounds could originate from the interaction of laser and protein. However, their formation mechanisms remain unclear [7].

Since femtosecond laser surgery is mainly based on multiphoton ionization and plasma mediated ablation [2], it is reasonable to hypothesize that the new fluorescent compounds could be formed via certain photochemical process induced in the interaction between femtosecond laser and tissue. However, it has been also reported that organic materials, such as protein [8,9], glucose and poly(vinyl alcohol) [10], can become fluorescent after thermal treatment. It should be noted that although femtosecond laser surgery is considered as a "non-thermal" procedure, the post-pulse equilibration is still a thermal process in nature. The ablation with a femtosecond laser of MHz repetition rate can cause an obvious heat accumulation effect increasing the local temperature in the treated areas [11,12]. Therefore, it is possible that the new fluorescent compounds originate from the heat accumulation effect of femtosecond laser ablation. It was reported that thermal treatment of biological samples could be used to produce highly fluorescent carbon dots [8]. Therefore, carbon dots might be responsible for the new fluorescence during femtosecond laser ablation. In addition, the new fluorescent compounds could also be the conjugated fluorophores produced via Maillard reaction, a chemical reaction between amino acids and sugars. In this study, we systematically examined these hypotheses and aimed to reveal the fundamental formation mechanism(s) of laser-ablation produced fluorescent compounds. In details, we first conducted imaging-guided fluorescence spectroscopy of laser-ablated biological samples (tissue and protein samples) to explore whether photochemical or thermal effect is responsible for the formation of new fluorescent compounds. Next, to address the thermal effect on the formation of new fluorescent compounds, we directly heated the biological samples at different temperatures and compared their fluorescence properties with the laser-ablated samples. Furthermore, we studied the chemical changes in the laser-ablated and thermal-treated samples using Raman spectroscopy and transmission electron microscopy. Finally, we investigated the role of Maillard reaction in the formation of new fluorescent compounds in biological samples. The experimental results of our study provided important insight into the formation mechanisms of fluorescent compounds produced by femtosecond laser in biological tissues.

2. Materials and methods

2.1 Imaging-guided fluorescence spectroscopy

Details of an integrated single-photon confocal and two-photon fluorescence spectroscopy imaging system have been described in our previous work [7]. Briefly, a femtosecond Ti:sapphire laser (Mira900-S, Coherent) with 140 fs pulse duration was used for two-photon fluorescence excitation and its second harmonic generation (SHG) from a β-barium borate (BBO) crystal was used for single-photon excitation. Since the single-photon excitation wavelengths were determined by the SHG range from 370 nm to 440 nm, the corresponding two-photon fluorescence excitation was set in the range from 740 nm to 880 nm. The two excitation beams were combined using a dichroic mirror and directed into a home-built upright laser scanning microscope with a descanned fluorescence collection configuration. A water immersion objective (UAPON 40XW340, 1.15 NA, Olympus) was used to focus the excitation beams into sample and collect the backward fluorescence signals. The fluorescence signals via both single- and two-photon excitation were analyzed by a spectrograph equipped with a 16 photomultiplier tube (PMT) array and a time-correlated single photon counting (TCSPC) module (PML-16-0 and SPC-150, Becker & Hickl). The system is capable to record signals of wavelengths ranging from 403 nm to 598 nm with a 13 nm spectral resolution and about 200 ps temporal resolution. Using this setup, we are able to study the time- and spectral-resolved single- and two-photon excited fluorescence emissions at the same location of sample.

Biomedical Optics EXPRESS

2.2 Raman spectroscopy and transmission electron microscopy

Raman spectra of laser-ablated and thermal-treated samples were measured using a commercial Raman spectrometer (Renishaw RM 3000). A 633 nm 5 mW helium–neon laser was focused on the samples with a microscope objective (50×, 0.55 NA). The integration time was ~50 seconds for a single Raman spectrum ranging from 1000 cm^{-1} to 3000 cm^{-1}. The fluorescence background of the Raman spectra was subtracted using an open source software (http://cares.wayne.edu/rp/download.html) [13]. For high-resolution transmission electron microscopy (HRTEM) experiments, the biological samples were finely ground in an agate mortar and dispersed in ethanol. A drop of dispersion was placed on a copper grid and visualized with the analytical HRTEMs (JEM ARM200F and FEI Talos F200X) equipped with energy-dispersive X-ray spectroscopy (EDX).

2.3 Sample preparation

The biological tissue samples were freshly isolated skin, muscle and brain from mice. The surgery procedure followed NIH guidelines and was approved by University Animal Ethical Committee. To prepare the protein samples, albumin (A7906, Sigma) was first dissolved in Milli-Q water at a concentration of 0.2 g/ml. A drop of solution was placed on a cover glass that was then put in a dry box until completely dried and an albumin film was formed on the cover glass. In the following study, half of the samples were ablated with a femtosecond laser at different powers and the rest were thermally heated with a hot plate at given temperatures from 100 °C to 400 °C for ~15 minutes. The laser-ablated and thermal-treated samples were characterized based on single- and two-photon fluorescence spectroscopy, Raman spectroscopy and HRTEM analysis, respectively. To study the contribution of individual amino acid to the formation of fluorescent compounds, lysine (L5501, Sigma), serine (S4500, Sigma), tryptophan (T0254, Sigma) and glycine (IB7019, IBI Scientific) were dissolved in Milli-Q water at a concentration of 0.2 g/ml (tryptophan cannot be fully dissolved at 0.2 g/ml and therefore its saturated solution was used). To study the effect of sugar in the fluorescence emission, glucose (G6142, Sigma) was dissolved in Milli-Q water at 0.2 g/ml and mixed with the albumin/amino acid solution (0.2 g/ml) at 1:1 ratio (v:v). The procedure for thermal treatment was the same as albumin samples.

3. Results and discussion

3.1 Formation of fluorescent compounds: photochemistry vs. thermal effects

Our previous work revealed that the laser ablated albumin and biological tissues (mouse skin, muscle and brain) exhibited similar fluorescence properties, suggesting that the fluorescent compounds in tissues could originate from the interaction between laser and proteins [7]. To understand how protein molecules become fluorescent via interaction with femtosecond laser, we ablated albumin samples along straight lines with laser power at different levels and then took the fluorescence images of the treated sites. Interestingly, we found that the fluorescent regions were not co-localized with the focal lines of ablation laser as shown in Fig. 1. They distributed in broad regions on both sides of the laser cutting lines defined by the laser focal spot of ~0.4 μm in diameter (740 nm laser, 1.15 NA objective). Similar results were also obtained in the femtosecond laser ablation in biological tissues (Appendix Fig. 10). These evidences demonstrate clearly that the fluorescent compounds are not produced via photon-induced chemical reaction which must be strictly confined in the laser focal volume.

Biomedical Optics EXPRESS

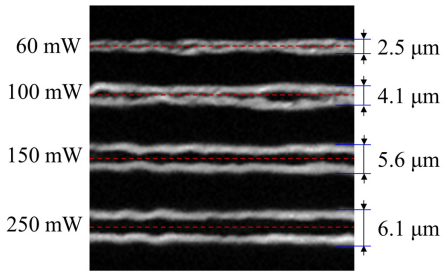

Fig. 1. Fluorescence image of line cutting in albumin sample by using 740 nm femtosecond laser with different powers. Red dashed line: laser cutting path. Laser cutting speed: 100 μm/s. Field of view: 50 μm × 50 μm.

In femtosecond laser ablation, the energetic plasma initiated by nonlinear multiphoton ionization in the laser focal region interacts with surrounding substances, resulting in the chemical bond breaking [2,11]. Therefore, the femtosecond laser surgery is generally considered as a non-thermal process. However, heating is a considerable effect in the post-pulse process, especially when the pulse interval of the laser is shorter than the heat diffusion time. The pulse interval of a standard Ti:sapphire femtosecond laser is 12.5 ns (80 MHz), which is far below the heat diffusion time out of the focal volume (typically ~1 μs) [11,12]. Heat generated from each pulse will accumulate in the focal volume and diffuse to the surrounding region, which can cause the temperature rise. Therefore, we hypothesize that the fluorescent compounds are produced by the laser heating effect and the heat diffusion results in the fluorescent regions much larger than the focal spot, particularly when the ablation laser power is high (Fig. 1 and Appendix Fig. 10). However, an interesting question is why there was no strong fluorescence observed from the regions close to laser focal spot.

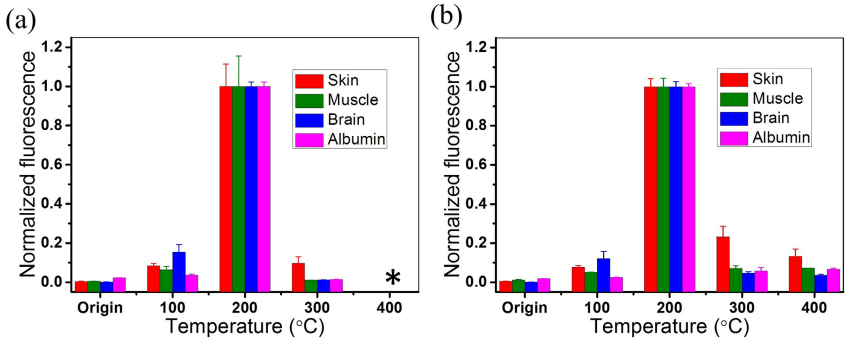

Fig. 2. Fluorescence intensities of mouse skin, muscle, and brain tissue and albumin without treatment (origin) and thermally treated at 100 °C, 200 °C, 300 °C and 400 °C. (a) Single-photon (440 nm) excited fluorescence intensities. (b) Two-photon (880 nm) excited fluorescence intensities. The intensities are normalized to the maximum (i.e., intensity at 200 °C) respectively. *: the signals from 400 °C-heated samples via single-photon excitation were too weak to be detected. Error bars represent ± SD.

To address the thermal effect on the formation of fluorescent compounds in biological samples, we directly heated tissues and albumin samples at different temperatures (ranging from 100 °C to 400 °C) and compared their fluorescence properties with laser ablated samples. As described in our previous work [7], the laser ablated samples possess a unique fluorescence property, exhibiting a large discrepancy in the emission spectra via single- and two-photon excitation. Therefore, we investigated the fluorescence properties of thermally treated samples using the same single- and two-photon fluorescence spectroscopy system. The fluorescence intensities of samples heated at different temperatures are shown in Fig. 2. We found that the samples became highly fluorescent when thermally treated at 200 °C. Their

Biomedical Optics EXPRESS

fluorescence emission spectra and lifetimes are displayed in Fig. 3. The peak of single-photon excited fluorescence emission spectra shifted from blue to red as the excitation wavelength redshifted and the two-photon excited fluorescence spectra all showed peaks at long wavelength range (> 510 nm). The fluorescence lifetimes were all approximately 1 ns and not sensitive to excitation wavelength. These fluorescence properties were consistent with those of the laser treated tissues. However, the fluorescence properties of the samples heated at other temperatures (room temperature, 100 °C, 300 °C and 400 °C, shown in Appendix Figs. 11-14) were much different from the laser-ablated samples and the samples directly heated at 200 °C. The results suggest that the fluorescent emission from the laser ablated tissue could be dominated by the tissue regions heated to about 200 °C.

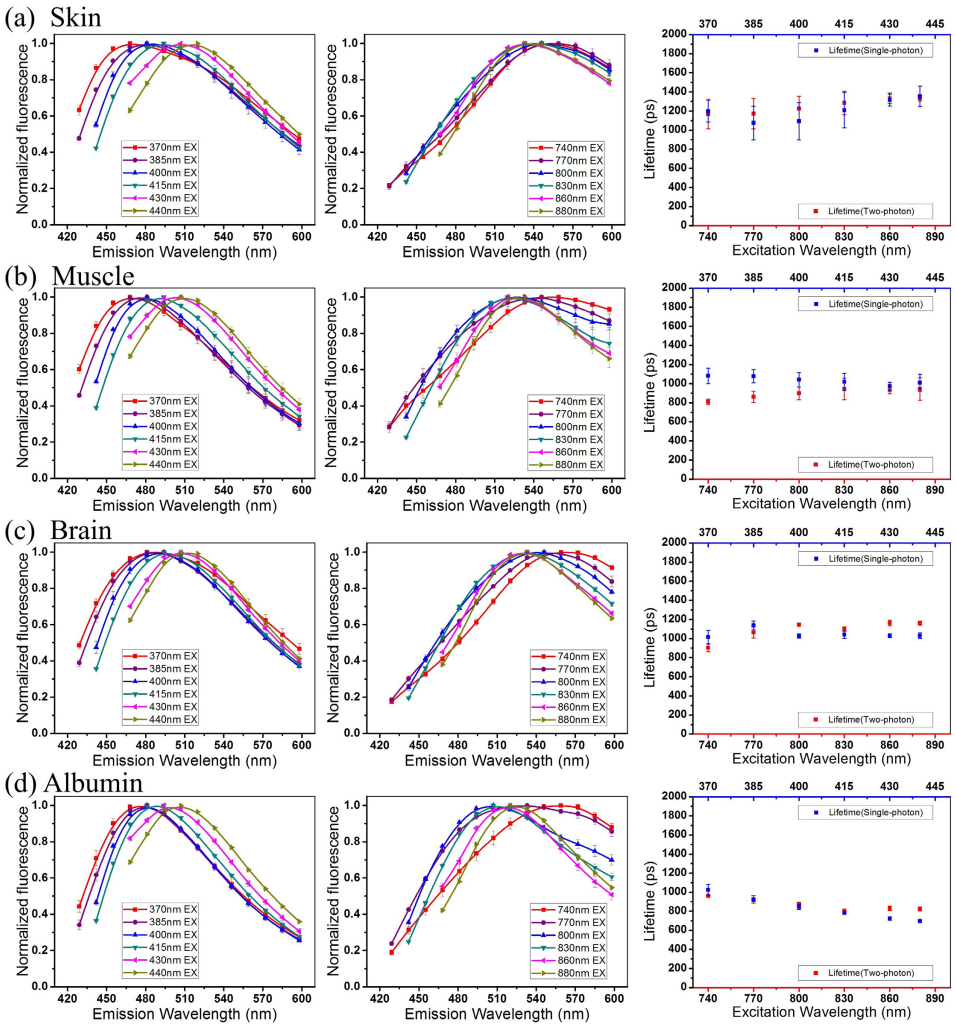

Fig. 3. Fluorescence properties of biological tissues and protein heated at 200 °C. (a) Mouse skin, (b) muscle, (c) brain tissue and (d) albumin. Left column: single-photon excited (370 nm to 440 nm) fluorescence emission spectra; middle column: two-photon excited (740 nm to 880 nm) fluorescence emission spectra; right column: single- and two-photon excited fluorescence lifetimes. Error bars represent ± SD.

During laser ablation, the heat diffusion process produces a temperature gradient from the laser focal spot, the heating center, to its surrounding region. We measured the fluorescence properties of the laser ablated samples at different distances away from the laser heating

Biomedical Optics EXPRESS

center and compared them with those measured from the samples thermally heated at different temperatures. As representative results, the properties of two-photon excited fluorescence from the laser-ablated and thermal-treated albumin samples are shown in Fig. 4. As can be seen in Fig. 4(a), although the temperature in tissue should decrease monotonically with the increase of distance away from the focal point of ablation laser due to the nature of heat diffusion, the intensity of fluorescence measured from the heating center was much lower than the surrounding region. Specifically, the signal intensity reached to the peak at the distance about 1.88 μm away from the laser focal point. This is consistent with the results from the thermally treated sample displayed in Fig. 4(d). The fluorescence intensity measured from the sample heated at high temperature (> 300 °C) were much lower than that heated at moderate temperature (~200 °C). The further analysis revealed that the fluorescence signal measured from the location close to the laser focal point had an obvious redshift and shorter lifetime (Fig. 4(b-c)), comparable to the sample thermally treated at a high temperature over 300 °C (Fig. 4(e-f)). However, the fluorescence spectrum and lifetime measured at 1.88 μm away from the laser focal point where the fluorescence intensity reached to peak was similar to those measured from the sample heated at 200 °C. In addition, the study with the laser-ablated and thermal-treated tissue samples also produced the similar results and the details are presented in Appendix Fig. 15. Based on the strong evidences, a conclusion can be drawn that the new fluorescent compounds originate from the laser heating effect and their major distributions are in the regions of heating temperature around 200 °C. Finally, it should be noted that we did not conduct the similar study with the single-photon fluorescence spectroscopy because the axial resolution of the homemade confocal system (~3.5 um) was not adequate to reject the interference from the out-of-focus signals.

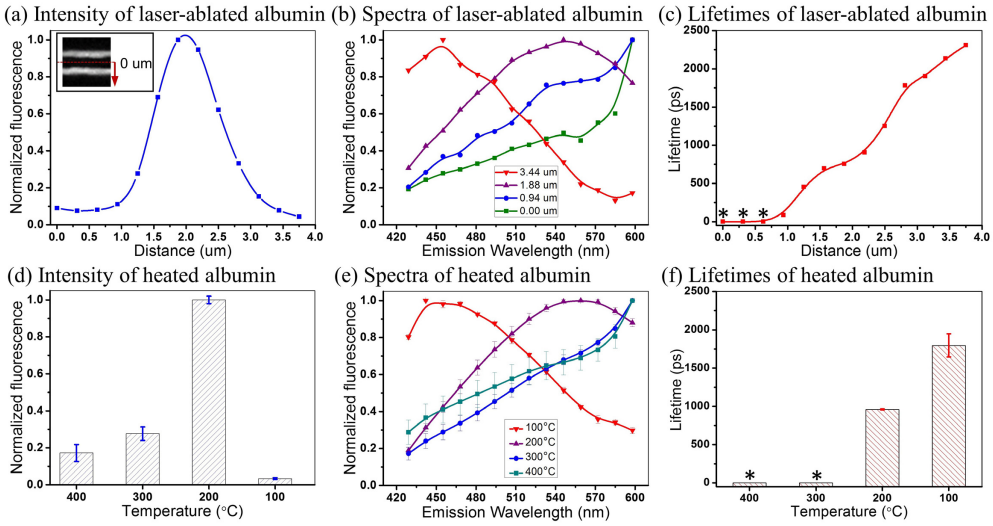

Fig. 4. Two-photon excited fluorescence properties of laser-ablated and thermal-treated albumin samples (740 nm excitation). Fluorescence intensity (a), spectra (b) and lifetimes (c) of the laser ablated albumin sample measured at different distances away from the focal point of ablation laser. Inset of (a) shows the image of laser ablated albumin sample (ablation laser power: 250 mW, details in Fig. 1). The fluorescence properties (intensities, spectra and lifetimes) were averaged along the dashed line and moved downwards from the center of laser ablation line. Fluorescence intensity (d), spectra (e) and lifetimes (f) of albumin sample heated at different temperatures. * The fluorescence decay curves are the same as system response (~200 ps), meaning that the lifetimes are much shorter than 200 ps. Error bars represent ± SD.

3.2 Raman spectroscopy and transmission electron microscopy

To identify the laser induced chemical changes in biological tissues, we first conducted Raman spectroscopy of the samples before and after laser ablation. As can be seen from the

Biomedical Optics EXPRESS

Raman spectra shown in Fig. 5, the original tissue samples before ablation showed two strong Raman peaks corresponding to CH_3 stretching (2930 cm^{-1}) and amide I vibration (1650 cm^{-1}), which are the signatures of protein molecules. After laser ablation, two strong peaks appeared at 1356 cm^{-1} and 1600 cm^{-1} in the Raman spectra of all samples, corresponding to the D and G bands of carbon materials. The D-mode vibration in carbon materials is from the sp^3 defect structure, and the G-mode is due to the E_{2g} in-plane vibration of sp^2 carbon [14]. These two Raman bands of carbon provide direct evidence that the femtosecond laser ablation process can induce carbonization in tissue, which has been reported in both biological tissues [15] and organic polymers [16,17].

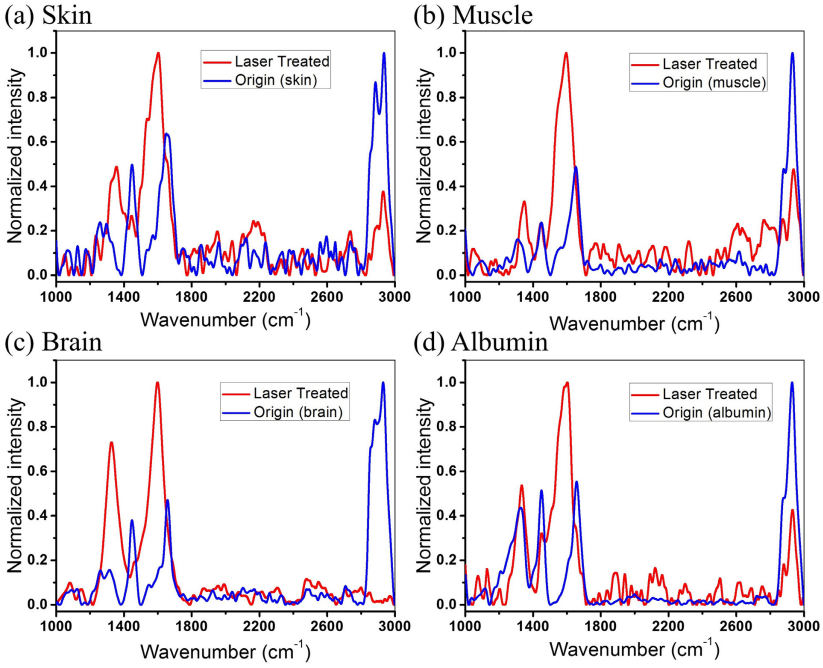

Fig. 5. Normalized Raman spectra of (a) mouse skin, (b) muscle, (c) brain tissue and (d) albumin before (blue line) and after (red line) laser ablation.

In the Raman spectroscopy study of thermally treated samples, we found that Raman spectra of samples heated at 100 °C, 200 °C and 300 °C did not show any Raman features of D and G bands. However, strong D and G bands appeared in the Raman spectra measured from all samples heated at 400 °C (Appendix Fig. 16). The results indicate that carbonization only occurs at high temperature, consistent with previous work which reported that protein can be carbonized when heated at temperatures higher than 350 °C [18]. However, the fully carbonized tissue by thermal treatment does not contribute to fluorescence emission because the fluorescence intensity measured from the samples heated at 400 °C is low and negligible in comparison with the samples heated at 200 °C (Fig. 2).

Recently, a new kind of highly fluorescent nanomaterial known as carbon dots has been reported [19–21]. Although their photoluminescence mechanisms are not fully understood, the carbon dots exhibit properties similar to highly fluorescent quantum dots. It has been reported that the carbon dots could be produced from the carbonization of many organic materials, such as carbohydrates [22], polymers [10], and proteins [8]. To address whether carbon dots were formed during laser ablation or thermal heating, we studied the nanostructures of all laser-ablated and thermal-treated samples using the high-resolution transmission electron microscopy (TEM). The representative results are shown in Appendix Fig. 17. As can be seen, the TEM images demonstrate that both laser-ablated and thermal-

Biomedical Optics EXPRESS

treated samples were dominated by amorphous bulk structures. When the heating temperature was higher than 300 °C, several amorphous nanoparticles were indeed observed in the biological tissues as shown in Fig. 6(a). However, as demonstrated in Fig. 6(b-c), the energy-dispersive X-ray (EDX) spectroscopy of the samples clearly confirmed that these amorphous nanoparticles were abundant with phosphorus and metals (e.g., magnesium and potassium), indicating that they could belong to phosphate salts. Therefore, we conclude that the fluorescent compounds are not carbon dots produced in carbonization. Based on the study of Raman spectroscopy and TEM, the fully carbonized tissue is not fluorescent and the carbonization process induced by laser ablation does not produce fluorescent carbon dots in tissue. This explains that in the fluorescence image of ablated tissue the region close to the focal point, where laser heating temperature reached to the maximal level, appears dark in comparison with surrounding regions (Fig. 1 and Appendix Fig. 10).

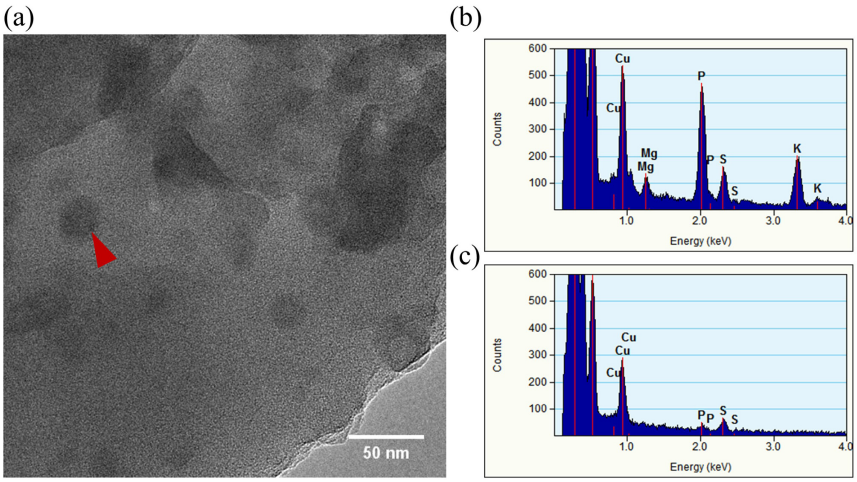

Fig. 6. TEM image and its EDX spectra in skin tissue heated at 400°C. (a) TEM image of several amorphous nanoparticles. (b) The EDX spectrum of an amorphous nanoparticle (red arrow head in (a)). (c) The EDX spectrum of amorphous bulk areas. Cu signals in (b) and (c) are from the copper grid used in the TEM measurement.

3.3 Maillard reaction

In heating experiments, the samples become browning first before carbonization with the increase of heating temperature (Appendix Fig. 18). Browning of heated tissue is a signature process attributed to the Maillard reaction that was first discovered in the mixture of sugar and amino acids. The most important functional groups in this reaction are carbonyl and amino group [23]. Briefly, the first step of Maillard reaction is condensation between carbonyl and amino group to form a Schiff base [23]. A variety of reactions then occur, forming the brown and fluorescent products such as melanoidins [24]. In addition, it was reported that carbonyl group, one of key reactants in Maillard reaction, can also be directly generated from proteins via thermal oxidation at the temperature over 180 °C [9], meaning that the amino group in proteins can react with their own carbonyl oxidation products to form the fluorescent compounds via Maillard reaction. In summary, the carbonyl group required by Maillard reaction are present in various sugars in tissues and can be also produced in thermally heated proteins. Although the detailed reactions are still not fully understood and the structures of fluorescent products have not been clearly identified [23,25], we hypothesize that the fluorescent compounds produced in the laser-ablated and thermal-treated samples could be directly related to the fluorescent products of Maillard reaction.

Amino acids are the basic building blocks of proteins in tissue. To explore which amino acids play an important role in the formation of fluorescent compounds via Maillard reaction,

Biomedical Optics EXPRESS

we directly heated the samples of four amino acids: lysine, serine, glycine, and tryptophan, respectively. They are the representatives of amino acids with polar charged, polar uncharged, nonpolar aliphatic and nonpolar aromatic side group [26]. We found that among these four amino acids, lysine and serine became browning after thermal treatment at 200 °C (Appendix Fig. 19(a)), but only lysine was highly fluorescent (Appendix Fig. 19(b-c)). The results are consistent with other work that lysine had the strongest fluorescence emission among 20 amino acids after heated at 180 °C [9]. This also confirms that Maillard reaction of certain amino acids can occur without presence of sugar with carbonyl group. In addition, we found that the fluorescence properties of 200 °C heated lysine sample shown in Fig. 7 were similar to the those measured from laser-ablated and 200 °C heated biological samples.

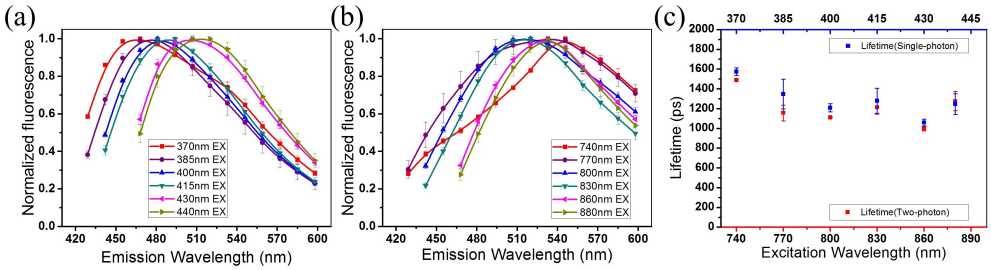

Fig. 7. Fluorescence properties of lysine heated at 200 °C. (a) Single-photon excited (370 nm to 440 nm) fluorescence emission spectra; (b) two-photon excited (740 nm to 880 nm) fluorescence emission spectra; (c) single- and two-photon excited fluorescence lifetimes. Error bars represent ± SD.

Next, we studied the effect of sugar on Maillard reaction and fluorescence emission of the reaction products. Glucose, the most abundant sugar in tissues in general, was used as the representative sugar in this study. We first heated the glucose and albumin at 100 °C. Both samples remained the same color and was not fluorescent (Fig. 8(a)). However, when the mixture of glucose and albumin was heated under the same condition, the sample became dark brown (Fig. 8(a)), similar to pure albumin sample was heated at 200 °C. The results indicate that the Maillard reaction occurred. The heated mixture became highly fluorescent, and the fluorescence intensity was comparable to the intensity of pure albumin heated at 200 °C (Fig. 8(b)). As shown in Fig. 9(a), the fluorescence emission spectra of the Maillard reaction products in the mixture of glucose and albumin also exhibited the excitation dependence via single-photon excitation and a large difference between single- and two-photon excitation, especially for short-wavelength excitation. Moreover, the fluorescence lifetimes were approximately 1.3 ns. All the fluorescence properties were similar to the directly heated samples at 200 °C and laser ablated samples.

Biomedical Optics EXPRESS

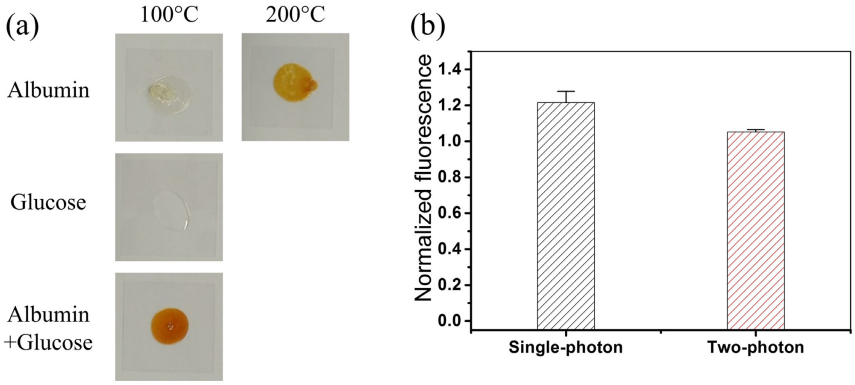

Fig. 8. (a) Photos of albumin, glucose and their mixture heated at different temperatures; (b) fluorescence intensity of albumin and glucose mixture heated at 100 °C. The single-photon (440 nm) and two-photon (880 nm) excited fluorescence intensities are normalized to the intensities of albumin heated at 200 °C, respectively. Error bars represent SD.

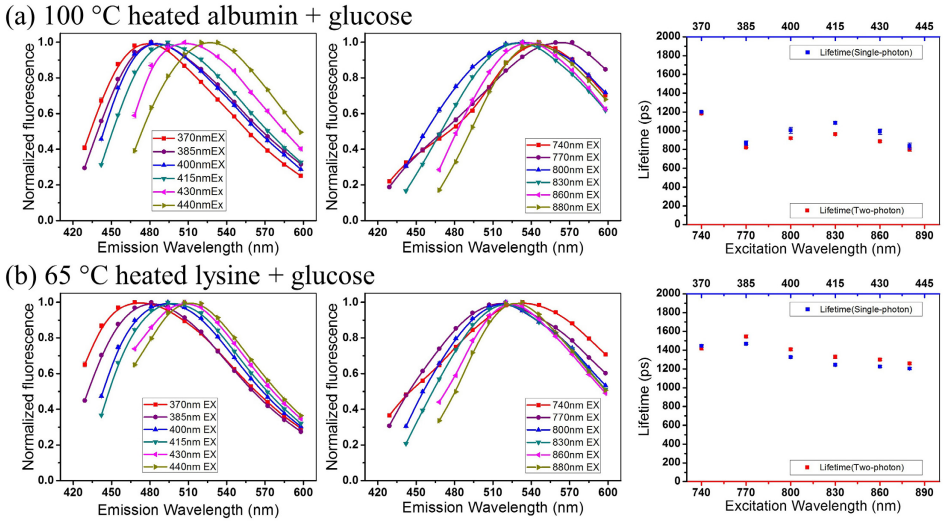

Fig. 9. Fluorescence properties of (a) mixture of albumin and glucose heated at 100 °C; (b) mixture of lysine and glucose heated at 65 °C. Left column: single-photon excited (370 nm to 440 nm) fluorescence emission spectra; middle column: two-photon excited (740 nm to 880 nm) fluorescence emission spectra; right column: single- and two-photon excited fluorescence lifetimes. Error bars represent ± SD.

We conducted similar experiments on the mixtures of amino acids and sugars. Specifically, four amino acids (lysine, serine, glycine, and tryptophan) were mixed with glucose respectively. Each mixture sample was then heated to different temperatures for fluorescence measurement. Except tryptophan, all other three amino acids mixed with glucose became brown and highly fluorescent after heated blow 100 °C (Appendix Fig. 20). The reason why tryptophan samples could not become fluorescent as other amino acids is unknown. As a representative result, the fluorescence properties of lysine and glucose mixture heated at 65 °C are shown in Fig. 9(b). The results demonstrate that sugar of carbonyl group can significantly enhance the Maillard reaction of proteins/amino acids and increase the production efficiency of fluorescent compounds at low heating temperature. Finally, in the study of browning process in protein and tissue samples, we found that the browning in biological tissues can start at a temperature as low as 100°C while the browning of pure protein requires the temperature close to 200 °C (Appendix Fig. 18). This should be due to the

Biomedical Optics EXPRESS

fact that tissue is not only rich in protein, but also contains sugar with reactive carbonyl group. The sugar can directly react with amino group in the protein via Maillard reaction resulting in the tissue browning at lower temperature.

4. Discussion and conclusion

In this work, we investigated the formation mechanism of new fluorescent compounds produced by femtosecond laser surgery in biological tissues. The experimental results demonstrate that they are produced via thermal effect based on post-pulse or pulse-interval thermal accumulation from the ablation laser of MHz repetition rate, instead of any photochemical process. We characterized the fluorescence properties of laser ablated and thermally heated biological samples including tissues and protein using the single-photon confocal and two-photon fluorescence spectroscopy. Our findings show that the laser-ablated and thermal-treated samples exhibit similar spectral and temporal fluorescence properties. Particularly, the fluorescence of laser ablated samples should be dominated by the signals from the region heated to about 200 °C. The appearance of D and G carbon bands in the Raman spectra indicates that carbonization occurs in the ablation process when laser power is at high level. This results in a dark region near the focal point. The TEM study confirms that the laser produced fluorescent compounds are not from highly fluorescent nanostructures. Finally, the findings of our study indicate that the fluorescent compounds are likely formed via Maillard reaction.

Although the detailed reaction process and fluorescent mechanisms remains unknown, the fluorescent centers of these compounds may be conjugated fluorophores produced via Maillard reaction. A recent study reported that even the degree of carbonization is very low when organic materials are heated at about 200 °C, there could be sufficient energy to crosslink chemical bonds to produce a new type of fluorescent compound [27]. The fluorescent compounds could be formed via crosslink from non-fluorophore units (called sub-fluorophores), such as C = O, C = N and N = O groups, instead of via typical conjugated fluorophore groups. The photoluminescence in sub-fluorophore is normally low, but can be increased through the chemical crosslinking or physical immobilization of polymer chains, which is named as the crosslink-enhanced emission (CEE) effect [27]. More recent experimental evidences also demonstrated that cocoon silk [28], glucose and glycine [29], and chitosan [30] can become fluorescent after heated at ~200 °C. Therefore, the crosslink of sub-fluorophores with the CEE effect could be responsible for the fluorescence emission from the laser-ablated biological samples. Further chemical analysis is required to identify the exact molecular structures of the new fluorescent compounds.

Appendix

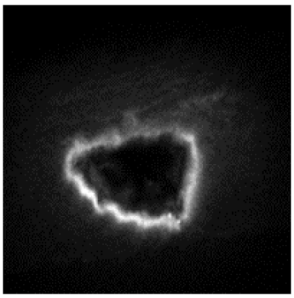

Fig. 10. Fluorescence image (740 nm excitation and 400-600 nm detection) of laser-ablated muscle tissue. The laser ablation was performed using a 740 nm femtosecond laser (250 mW) focused at a fixed point for 2 seconds. Field of view: 35 μm × 35 μm.

Biomedical Optics EXPRESS

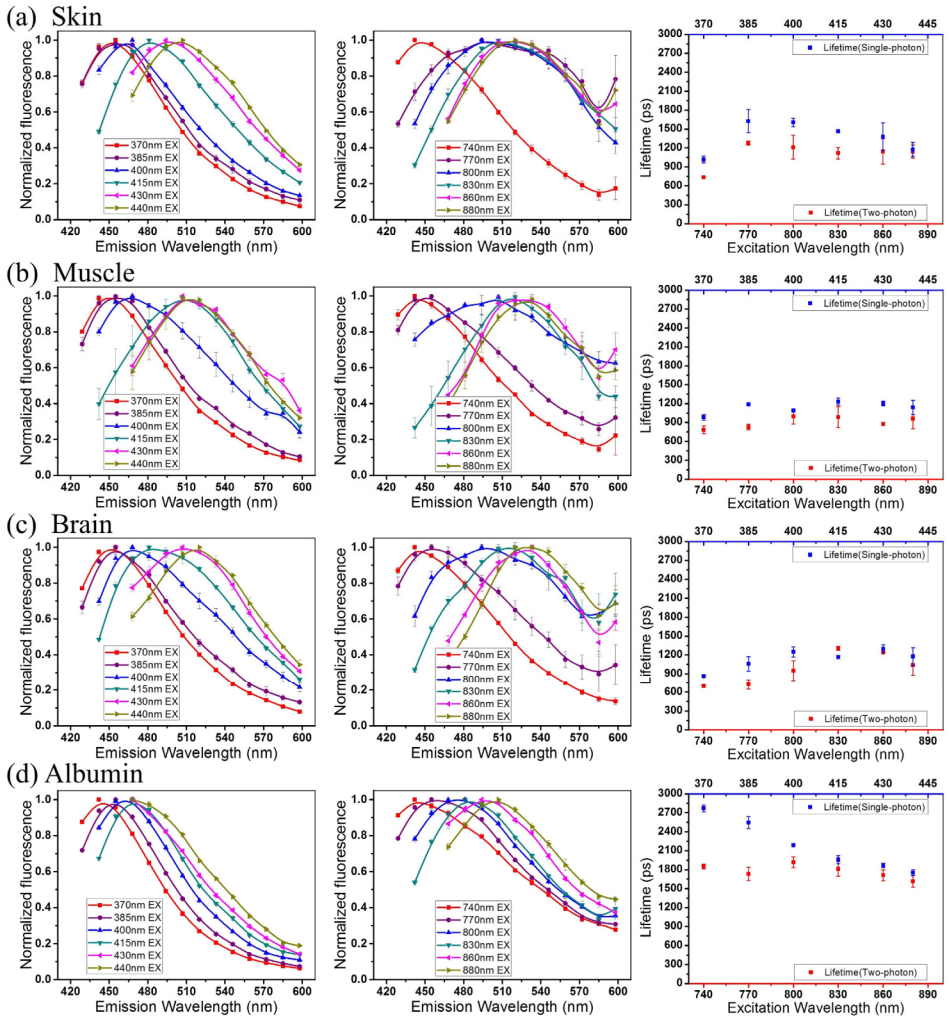

Fig. 11. Fluorescence properties of biological tissues and protein before laser ablation and heating treatment. (a) Mouse skin, (b) muscle, (c) brain tissue and (d) albumin. Left column: single-photon excited (370 nm to 440 nm) fluorescence emission spectra; middle column: two-photon excited (740 nm to 880 nm) fluorescence emission spectra; right column: single- and two-photon excited fluorescence lifetimes. Error bars represent ± SD.

Biomedical Optics EXPRESS

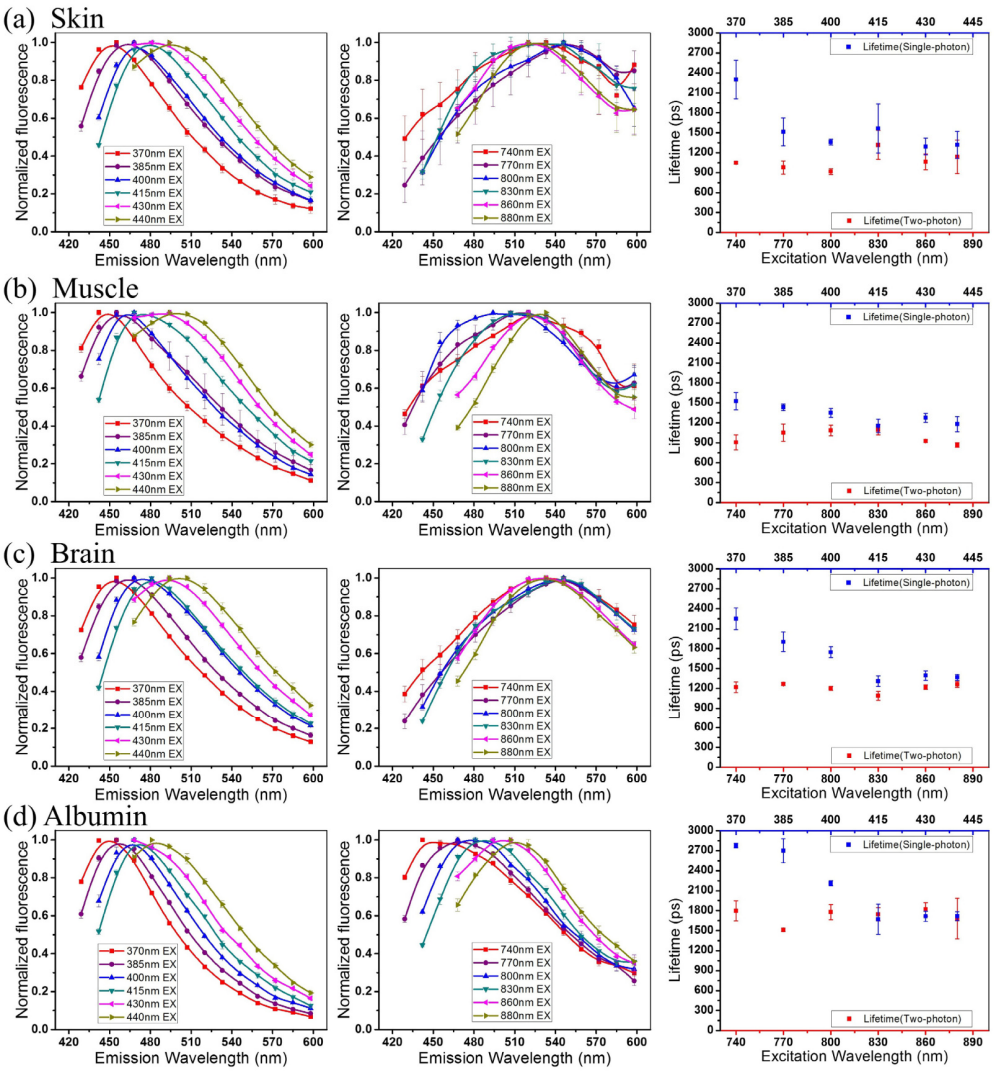

Fig. 12. Fluorescence properties of biological tissues and protein heated at 100 °C. (a) Mouse skin, (b) muscle, (c) brain tissue and (d) albumin. Left column: single-photon excited (370 nm to 440 nm) fluorescence emission spectra; middle column: two-photon excited (740 nm to 880 nm) fluorescence emission spectra; right column: single- and two-photon excited fluorescence lifetimes. Error bars represent ± SD.

Biomedical Optics EXPRESS

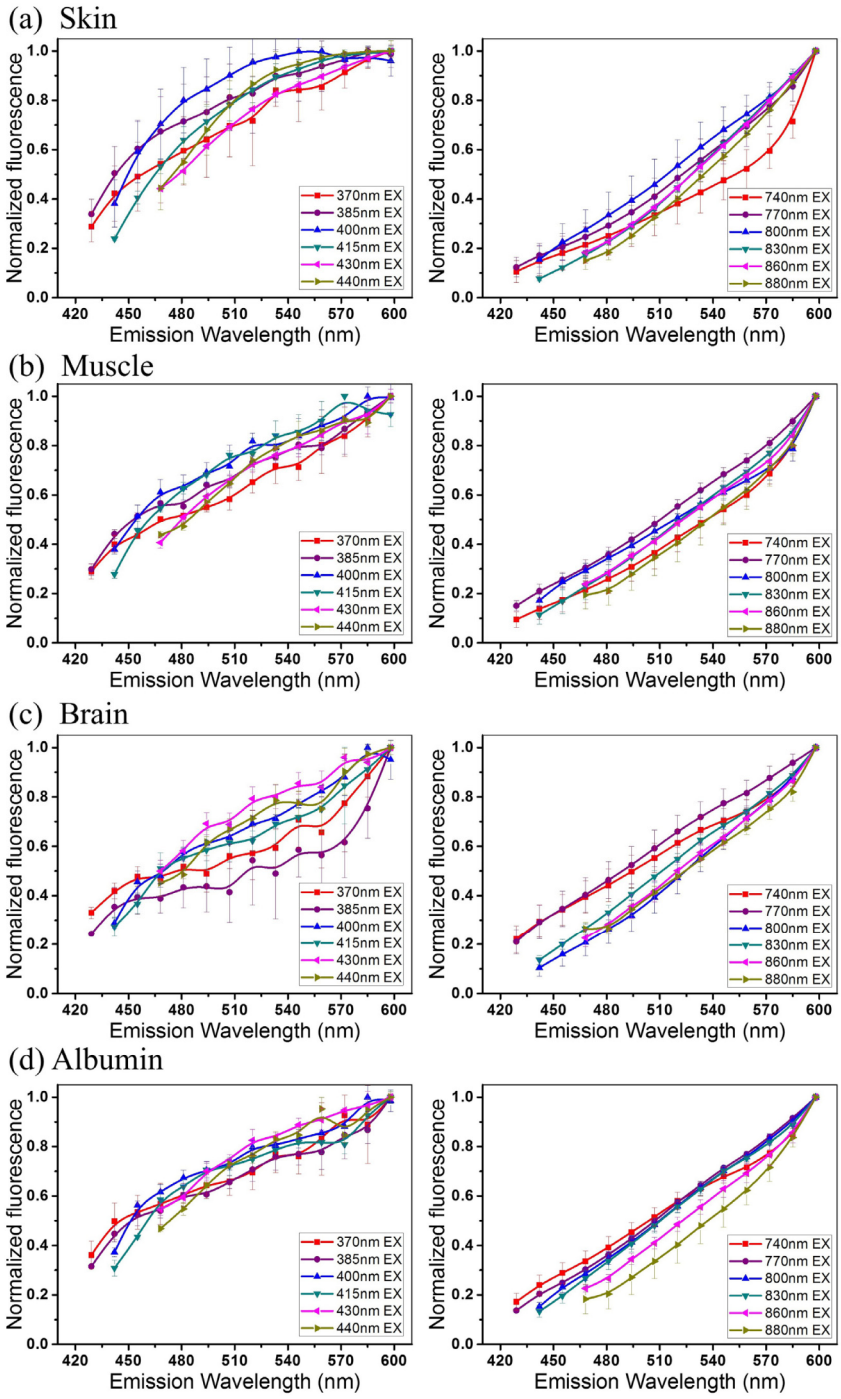

Fig. 13. Fluorescence properties of biological tissues and protein heated at 300 °C. (a) Mouse skin, (b) muscle, (c) brain tissue and (d) albumin. Left column: single-photon excited (370 nm to 440 nm) fluorescence emission spectra; right column: two-photon excited (740 nm to 880 nm) fluorescence emission spectra. The fluorescence decay curves are the same as system response (~200 ps), meaning that the lifetimes are much shorter than 200 ps. Error bars represent ± SD.

Biomedical Optics EXPRESS

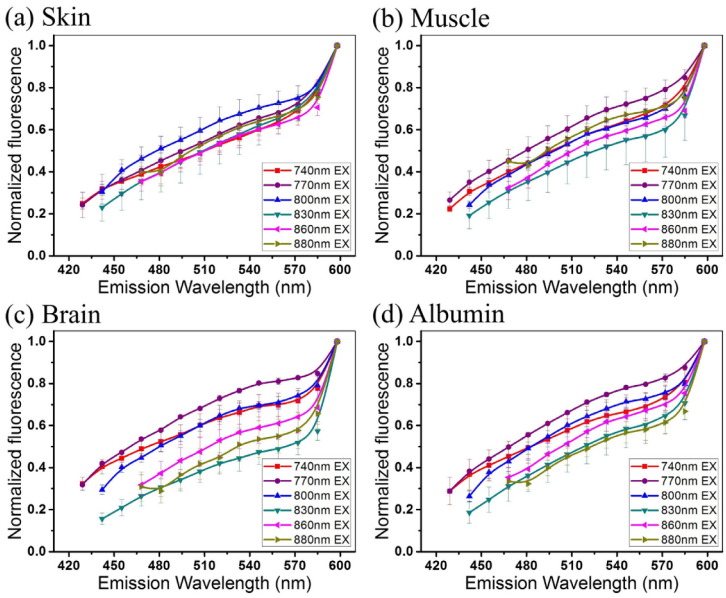

Fig. 14. Two-photon excited (740 nm to 880 nm) fluorescence emission spectra of biological tissues and protein heated at 400 °C. (a) Mouse skin, (b) muscle, (c) brain tissue and (d) albumin. The signals via single-photon excitation were too weak to be detected. The fluorescence decay curves are the same as system response (~200 ps), meaning that the lifetimes are much shorter than 200 ps. Error bars represent ± SD.

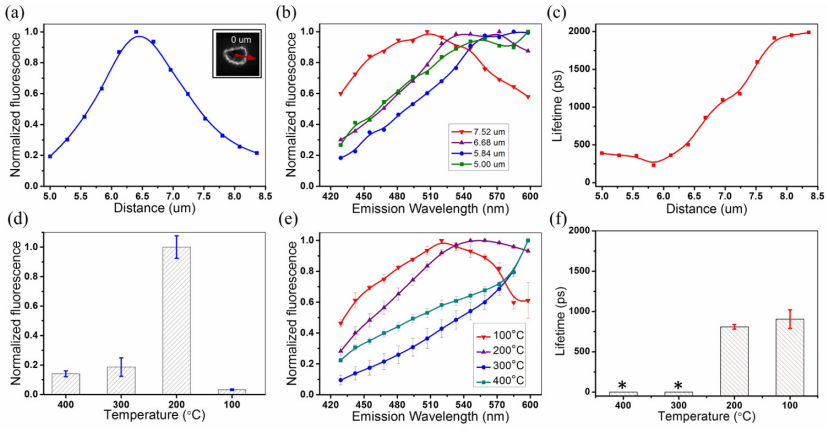

Fig. 15. Two-photon excited fluorescence properties of laser-ablated and thermal-treated mouse muscle tissue (740 nm excitation). (a) Fluorescence intensity as a function of distance from the focal spot of ablation laser (Inset shows the image of laser ablated muscle tissue and details are shown in Fig. 10). Fluorescence spectra (b) and lifetimes (c) of the laser ablated muscle sample measured at different distances away from the focal point of ablation laser. Fluorescence intensity (d), spectra (e) and lifetimes (f) of the muscle sample heated at different temperatures. *The fluorescence decay curves are the same as system response (~200 ps), meaning that the lifetimes are much shorter than 200 ps. Due to the inhomogeneity of heat diffusion in muscle tissue, the laser produced fluorescent compounds are not as even distributed as in albumin sample (Fig. 4). In addition, endogenous fluorophores such as NADH caused interference to the characterization of fluorescence properties in the region far from the heating center. This results in that fluorescence properties in the region far away from the heating center are not identical to the low temperature heated samples (100 °C). Error bars represent ± SD.

Biomedical Optics EXPRESS

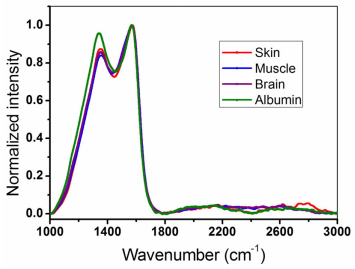

Fig. 16. Raman spectra of mouse skin, muscle, brain tissue and albumin heated at 400 °C.

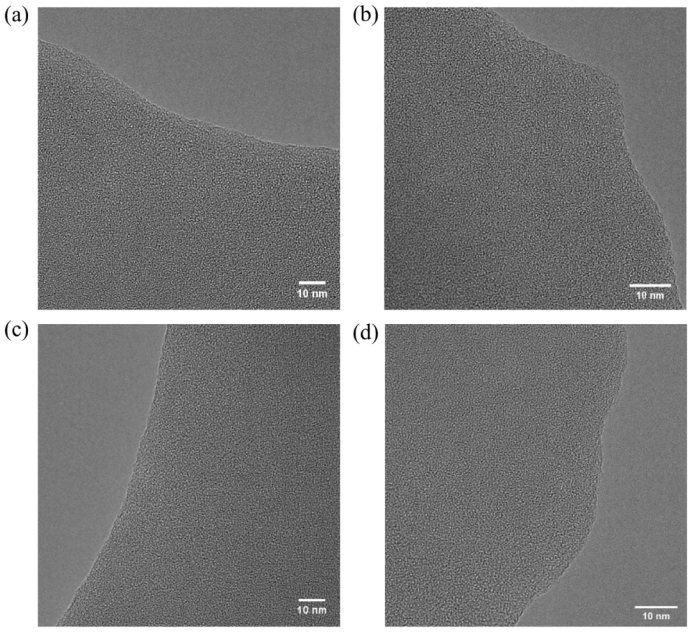

Fig. 17. TEM images of (a) skin, (b) muscle, (c) brain tissue and (d) albumin heated at 200 °C.

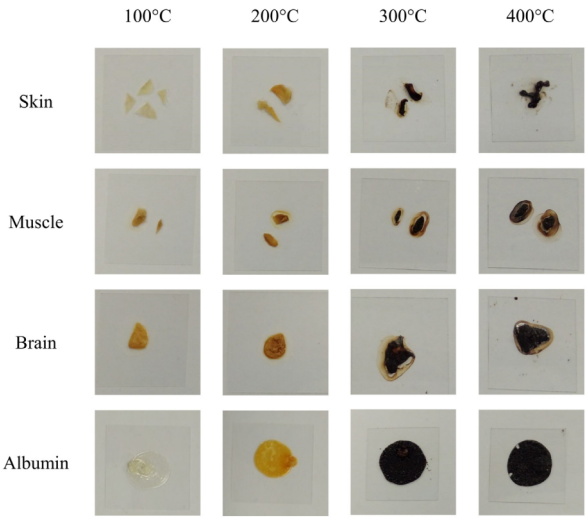

Fig. 18. Photos of biological tissues and albumin heated at different temperatures.

Biomedical Optics EXPRESS

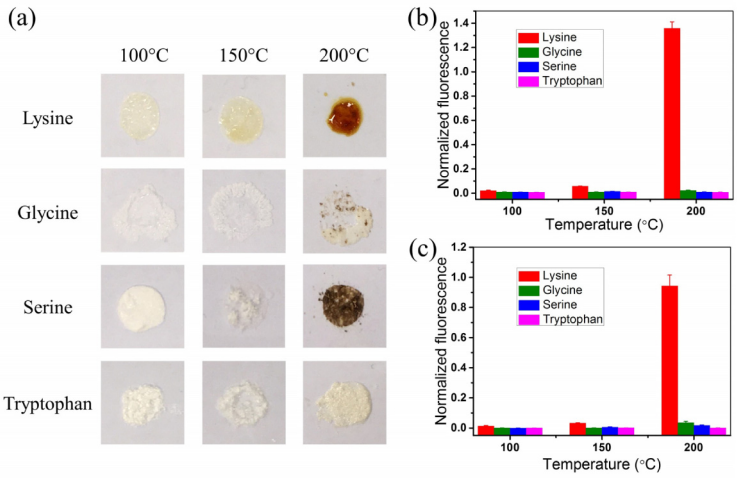

Fig. 19. Photos and fluorescence intensities of amino acid samples heated at different temperatures. (a) Photos of amino acid samples; (b) single-photon (440 nm) excited fluorescence intensities; (c) two-photon (880 nm) excited fluorescence intensities. All single- and two-photon fluorescence intensities are normalized to the intensities of albumin heated at 200 °C respectively. Error bars represent ± SD.

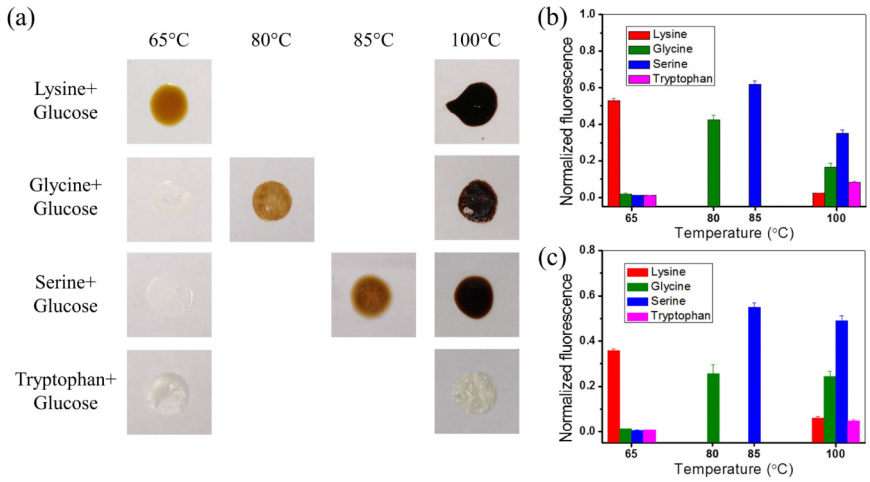

Fig. 20. Photos and fluorescence intensities of amino acid and glucose samples heated at different temperatures. (a) Photos of samples heated at different temperatures; (b) single-photon (440 nm) excited fluorescence intensities; (c) two-photon (880 nm) excited fluorescence intensities. All single- and two-photon fluorescence intensities are normalized to the intensities of albumin heated at 200 °C respectively. Error bars represent ± SD.

Funding

Hong Kong Research Grants Council (662513, 16103215, 16148816, T13-607/12R, AOE/M-09/12, C6002-17G); Hong Kong University of Science & Technology (RPC10EG33).

Disclosures

The authors declare that there are no conflicts of interest related to this article.